Published in final edited form as:
Pediatr Dev Pathol. 2013 ; 16(6): 405–414. doi:10.2350/13-08-1359-OA.1.

Microtomographic Analysis of Lower Urinary Tract Obstruction

Joseph R. Siebert[1,2,3,4,*], **Kenneth J. Smith**[3], **Liza L. Cox**[3], **Ian A. Glass**[3,5,6], and **Timothy C. Cox**[3,5,7]

[1]Department of Laboratories, Seattle Children's Hospital, Seattle, WA, USA

[2]Department of Pathology, University of Washington, Seattle, WA, USA

[3]Department of Pediatrics, University of Washington, Seattle, WA, USA

[4]Center for Clinical and Translational Research, Seattle Children's Research Institute, Seattle, WA, USA

[5]Center for Developmental Biology and Regenerative Medicine, Seattle Children's Research Institute, Seattle, WA, USA

[6]Department of Medical Genetics, Seattle Children's Hospital, Seattle, WA, USA

[7]Department of Anatomy and Developmental Biology, Monash University, Clayton, VIC, Australia

Abstract

Prenatal obstruction of the lower urinary tract may result in megacystis, with subsequent development of hydro-ureter, hydronephrosis, and renal damage. Oligo- or anhydramnios, pulmonary hypoplasia, and prune belly syndrome are lethal consequences. Causes and mechanisms responsible for obstruction remain unclear but might be clarified by anatomic study at autopsy. To this end, we employed 2 methods of tomographic imaging—optical projection tomography and contrast-enhanced microCT scanning—to elucidate the anatomy of the intact urinary bladder and urethra in 10 male fetuses with lower urinary tract obstruction. Images were compared with those from 9 age-matched controls. Three-dimensional images, rotated and sectioned digitally in multiple planes, permitted thorough examination while preserving specimens for later study. Both external and internal features of the bladder and urethra were demonstrated; small structures (ie, urethral crest, verumontanum, prostatic utricle, ejaculatory ducts) were seen in detail. Types of obstruction consisted of urethral atresia (n = 5), severe urethral stenosis (n = 2), urethral diaphragm (n = 2), or physical kinking (n = 1); classic (Young type I) posterior urethral valves were not encountered. Traditional light microscopy was then used to verify tomographic findings. The prostate gland was hypoplastic or absent in all cases; in 1, prostatic tissue was displaced inferior to the verumontanum. Findings support previous views that dissection may produce valve-like artifacts (eg, bisection of an obstructing diaphragm) and that deformation of an otherwise normal urethra may result in megacystis. The designation "posterior urethral valves" should not be used as a generic expression of urethral obstruction unless actual valves are demonstrated.

Keywords

lower urinary tract obstruction; microCT scanning; optical projection tomography; posterior urethral valves; prune belly syndrome; urethral atresia

*Corresponding author, joseph.siebert@seattlechildrens.org.

INTRODUCTION

Lower urinary tract obstruction (LUTO) carries serious consequences for the developing fetus. In the condition, which affects males in the great majority of instances, urethral stenosis or atresia, posterior urethral valves, and other forms of bladder outlet obstruction result in megacystis, hydroureter, and hydronephrosis, with subsequent renal parenchymal damage and renal failure. The ensuing development of oligo- or anhydramnios leads to pulmonary hypoplasia and oligohydramnios sequence, often with severe arthrogryposis (Potter and Pena-Shokeir phenotypes). Pronounced megacystis, often with urinary ascites, is associated with hypoplasia, degeneration, or complete attenuation of abdominal muscles and manifests as prune belly syndrome. The constellation of anomalies is associated with severe morbidity and often perinatal or postnatal mortality.

Through careful imaging studies in the clinical setting (eg, voiding cystourethrography) or dissection at autopsy, several types of obstruction have been described and classified [1,2]. The Young classification of posterior urethral valves, for example, consists of 3 categories: type I, posterior urethral valves that extend below (distal to) the verumontanum; type II, valves that extend above (proximal to) the verumontanum; and, type III, a transverse membrane or diaphragm that obstructs the urethral lumen. The classification has engendered debate but provides a framework that is useful for discussion and will be used in this study.

Anatomic distinctions carry some import. From a clinical point of view, treatment, when instituted, may depend upon the type of obstruction. Some of these types (posterior urethral valves and urethral stenosis or atresia) may recur in families [3,4]. From a research perspective, etiology and pathogenesis remain obscure. It is unclear, for example, if the sequence of events described above is operational in every case or if more generalized mesodermal defects affect bladder, bladder outlet, and/or abdominal wall musculature independently. Some do not believe that the Young type II valves exist in the clinical setting, while others hypothesize that the obstructing membrane (type III) may rupture prenatally or be damaged by autopsy examination or clinical treatment, resulting in the bivalved appearance of the other types [5].

Unfortunately, the precise lesions responsible for bladder outlet obstruction can be challenging to diagnose, whether by clinical imaging or anatomic means. Standard prenatal ultrasonography serves as a valuable screening tool for identifying dilated bladder and posterior urethra but does not allow visualization of actual valves [6]. Interpretation of postnatal imaging can be challenging as well [7,8]. Postmortem dissection may produce artifacts, yielding an inaccurate diagnosis. Incising an obstructing urethral membrane (type III), for example, can produce the erroneous appearance of posterior urethral valves (type I or II). For this reason, some autopsy pathologists have suggested that the obstructed urethra be examined as intact as possible, by unroofing the anterior wall of the bladder and posterior urethra or by microscopic means [9,10]. Histologic examination is time consuming and expensive, is limited to a single plane, and requires precise orientation of tissue and, in many instances, serial sectioning; it can be performed only once per specimen.

In an effort to better understand the anatomy of the normal and obstructed urethra, we have employed 2 microtomographic techniques: optical projection tomography (OPT) and microCT scanning. The former is a modality that uses visible, infrared, and ultraviolet light options to image small, translucent specimens [11,12]. The latter is a form of X-ray–based computed tomographic (CT) scanning employed in the study of small specimens composed of either soft tissue or bone [13]. For each, dedicated software is used to reconstruct tomographic images in 3 dimensions for additional study. In both methods, specimens remain intact during examination, can be visualized in detail as virtual 2-dimensional slices

in any plane or in 3 dimensions, and are available for subsequent light microscopy if desired. The results of examination by OPT or microCT are presented below for a series of control and affected male fetuses.

METHODS

In this study, a total of 9 control and 10 abnormal specimens were acquired at autopsy and examined in the following manner. Five control and 3 abnormal specimens consisting of intact lower urinary bladder and prostatic urethra were examined by OPT. They were fixed in formalin at the time of autopsy and subsequently embedded in low–melting point agarose gel, dehydrated in methyl alcohol, cleared with 1:2 benzyl alcohol:benzyl benzoate (BABB), and scanned under ultraviolet light (filter 475 nm) to capture autofluorescence (Table 1). Four additional control and 7 abnormal specimens were fixed in formalin, immersed in phosphotungstic acid with hematoxylin (PTAH) for several days, rinsed, and examined by microCT scanning (Table 1). Smaller, translucent specimens were imaged by OPT and larger, more opaque ones by microCT.

All bladders were imaged at the Seattle Children's Research Institute's Small Animal Tomographic Imaging Facility. For PTAH-stained bladders, imaging was performed using a model 1076 microCT (Skyscan, Kontich, Belgium). Scans were performed at 35 μm resolution using the following settings: 65 kV (~150 μA), 0.5 mm aluminum filter, 160 ms exposure with 3 frame averaging, and a rotation step of 0.7°. For the smaller specimens, imaging was performed based on tissue autofluorescence using a model 3001M OPT at a pixel resolution of 1024 × 1024 and digital zoom to between 5.6 and 9.3 μ depending on the size of the bladder. In preparation for scanning, bladders were embedded in 1.1% low–melting point agarose, dehydrated in methanol, and cleared in BABB.

For both OPT and microCT scans, raw image data were reconstructed using NRecon (V 1.6) software (Skyscan); virtual sections were examined independently and also rendered for viewing as a 3-dimensional volume using Bioptonics Viewer v2 and Drishti v2.0 software (http://sf.anu.edu.au/Vislab/drishti).

After imaging, specimens were examined by light microscopy as a means of comparing and validating findings. The research was carried out with approval of the Seattle Children's Institutional Review Board.

RESULTS

By both OPT and microCT, the external and internal features of the urinary bladder and posterior urethra are readily visualized in single planes or via 3-dimensional rendered images (Figs. 1–7). The latter can be rotated at will and levels subtracted, effectively permitting "virtual sectioning" in any plane. Small structures, including the urethral crest, verumontanum, and its components (ie, prostatic utricle and ejaculatory ducts) can be seen in detail (Figs. 1,4).

In 2 cases, OPT revealed urethral atresia, and in 1, a type III obstructing diaphragm (Table 1). Because the technique is light based, it carries some limitation with regard to specimen size and depth of field. In examining Figures 1–3, it is apparent that only a portion of the specimen appears to be in focus. This is due to background noise (reduced autofluorescence secondary to tissue thickness), and so specimens need to be examined by varying the plane of imaging, in a manner akin to rocking the focus in light microscopy.

By microCT, severe urethral stenosis or atresia was identified in 4 cases; a tortuous, stenotic urethra was seen in 1 case; and a type III obstructing diaphragm was seen in 2 cases (Table

1). In 1 case of VACTERL association (a nonrandom grouping of vertebral, anal, cardiac, tracheo-esophageal, radial or renal, and limb anomalies), atypical urethral stenosis was associated with ectopic ureters, seminal vesicles, and rectovesical fistula. Depth of field was not an issue in this X-ray–based technique, because the stain provides sufficient contrast throughout the specimen.

The posterior urethra was significantly dilated by both ultrasonography (“keyhole sign”) and autopsy examination in cases of urethral atresia, type III obstructing diaphragm, and physiologic kinking (Table 1).

Subsequent light microscopy using serial sections confirmed the microtomographic diagnosis in 9 of 10 cases (Table 2). In 1, a severely stenotic urethral lumen was seen by light microscopy but had appeared to be atretic by microtomography. Prostatic tissue was hypo-plastic or absent in all cases; in 1, prostatic tissue was present significantly distal to the verumontanum (Table 2). The obstructing diaphragm observed in 2 cases was composed of a thin band of urothelial cells supported by underlying connective tissue (Fig. 5E).

DISCUSSION

Optical projection tomography is a form of light-based, tomographic microscopy applicable to the study of small, translucent specimens (Table 3). During computer-driven scanning, tissues undergo 360° of rotation, with acquisition of digital images every 0.7°. The resulting images are then typically reconstructed using dedicated software into a 3-dimensional dataset that can be examined in any virtual plane of section, or as a 3-dimensional–rendered volume. Because OPT is nondestructive, specimens remain intact throughout imaging and are thus available for additional forms of examination, including light microscopy. Optical projection tomography is faster, is less expensive, and offers higher resolution than micro-MRI and can image larger specimens than confocal microscopy.

MicroCT is a form of computerized tomographic imaging designed for the radiographic examination of small specimens. MicroCT has certain advantages over OPT, chiefly that specimens can be of greater size and opacity (Table 3). Prior to scanning, soft tissues must be stained with a heavy metal to provide suitable differential contrast to the tissue.

Microtomography is a powerful tool for the study of small specimens. As such, it offers a fresh way to address questions of both clinical and research interest, perhaps especially those involving anatomically complex malformations of the cardiovascular, respiratory, genitourinary, biliary, or central nervous systems. In the present study, OPT and microCT provided vivid demonstrations of the external and internal features of the intact fetal and perinatal urinary bladder and posterior urethra, thus augmenting classic autopsy and facilitating postmortem diagnosis.

Severe urethral stenosis or atresia was diagnosed in 7 of 10 cases. An obstructive diaphragm (Young type III valve) was identified in 2 cases. A tortuous but otherwise nonobstructed posterior urethra in 1 case supports the opinion that isolated kinking can cause significant bladder outlet obstruction [10,14]. In 1 atypical case, multiple anomalies of the urinary bladder, urethra, and rectum were identified in an infant with VACTERL association. These changes were difficult to demonstrate at autopsy but readily seen by microCT. Such anomalies have been reported previously in this condition [15,16].

This study supports others’ opinion that anatomic diagnosis is most reliable when based upon examination of the intact urethra. If the urethras in our cases of obstructive diaphragm had been examined by traditional dissection, they would have been opened with scissors and the diaphragm bisected, yielding an incorrect diagnosis of separate, type I posterior urethral

valves. In fact, no classic type I valves were encountered in this study. This was somewhat surprising, and the reason is unclear. Given our experience prior to microtomography, we would have expected to see instances of type I valves. Given the small number of cases, we cannot rule out sampling error. However, it also seems possible that some of the type I valves we have diagnosed in the past were created artifactually, at autopsy or clinically [5]. It is also possible that the type III obstructing diaphragm is more common than is realized [9]. Still another possibility, as others have suggested, is that the type III obstructing diaphragm may rupture spontaneously later in gestation, giving the appearance of type I or II valves. In our previous experience with type I valves, infants were more likely to be older than those reported in this study and so the possibility of rupture of obstructive diaphragms remains an intriguing hypothesis.

After examination by microtomography, specimens can be examined by traditional light microscopy. To reach definitive conclusions, this requires serial sectioning, a tedious and expensive prospect that involves precise orientation and cutting, followed by reorientation of anatomic relationships. Each of the 10 cases of obstruction in the present study required hundreds of histologic sections to depict the lesions completely and of course hours of time spent in preparation and examination of slides. In 9 of our 10 cases, light microscopy yielded diagnoses that were identical to those reached by OPT or microCT. In 1 case of urethral atresia (case 4) diagnosed by microCT, a subsequent finding of severe urethral stenosis was made by light microscopy. The residual lumen was tiny, with almost completely opposed mucosal surfaces, and not seen during microtomographic scanning. For purposes of validation, it is important to make this distinction. From a physiologic and perhaps pathogenetic standpoint, however, the importance of distinguishing severe urethral stenosis from urethral atresia is less clear.

In all cases, the prostate gland was hypoplastic or could not be identified despite serial sectioning. In 1 instance (case 3), prostatic tissue was present in sections of urethra taken distal to the verumontanum. The reason for this is not understood. It is possible that severe dilatation of the prostatic urethra occurs proximal to the level of the prostate gland or may result in inferior displacement of the gland. It is also possible that a more generalized developmental error results in displacement of the gland. The relationship of the prostate gland to urethral obstruction is one of continuing interest and requires further study.

The anatomic delineation of these lesions has ramifications for both clinical and pathology practice. The prenatal ultrasonographic diagnosis of LUTO relies significantly upon visualizing a dilated urinary bladder and often a dilated, keyhole-shaped posterior urethra. In the present study, dilatation of the posterior urethra was diagnosed both clinically and at autopsy in cases of urethral atresia, type III obstructing diaphragm, and urethral deformation. This observation affirms the conclusion of some ultrasonographers that the keyhole sign is not predictive of classic posterior urethral valves [17]. Unfortunately, the diagnosis of “posterior urethral valves” is sometimes made without positively identifying valve tissue. Type I posterior urethral valves cannot be differentiated from other forms of obstruction (eg, urethral diaphragm, atresia) by traditional ultrasonography, and diagnosis can be erroneous if based upon the observation of megacystis and echoic kidneys alone [14,17–19]. We recommend that clinical diagnosis in this context be expressed in more generic terms (eg, “bladder outlet obstruction,” “LUTO”), recognizing that the resolving power of current ultrasonography is insufficient to permit a more precise anatomical diagnosis. This shortcoming may change as technology evolves.

This approach will presumably have consequences for epidemiologic understanding as well. Estimates of the incidence of particular types of posterior urethral valves vary substantially and have been hampered by the reliability of diagnosis. The recent literature, for example,

contains numerous clinical reports of posterior urethral valves, often indicating that type I valves are the most common variant. This may be inaccurate when diagnoses are based upon prenatal ultrasonographic identification of a dilated bladder and posterior urethra without subsequent anatomic confirmation of valves.

These issues will be clarified by the careful workup of additional cases. Newer forms of ultrasonography may provide higher resolution [21] while pathologists continue to exercise great care in postmortem workups. The anatomic delineation of bladder outlet obstruction should further the understanding of pathogenesis and etiology. This, in turn, may influence in utero therapy, aid in counseling families, and contribute to the ultimate prevention of this serious anomaly.

Acknowledgments

This research was supported in part by a grant from the Eunice Kennedy Shriver National Institute of Child Health & Human Development (NIH Award Number 5R24HD000836).

We are grateful to Leigh Martin for assistance in preparing specimens for OPT and to Raj P. Kapur, MD, PhD, for ongoing collaboration.

References

1. Young HH, Frontz WA, Baldwin JC. Congenital obstruction of the posterior urethra. J Urol. 1919; 3:289–365.
2. Stevens, FD. Anus and Genito-Urinary Tracts. Edinburgh: E. & S. Livingstone Ltd; 1963. Congenital Malformations of the Rectum.
3. Schreuder MF, van der Horst HJ, Bökenkamp A, et al. Posterior urethral valves in three siblings: a case report and review of the literature. Birth Defects Res A Clin Mol Teratol. 2008; 82:232–235. [PubMed: 18240166]
4. Siebert JR, Walker MPR. Familial recurrence of urethral stenosis/atresia. Birth Defects Res A. 2009; 85:715–719.
5. Kajbafzadeh A. Congenital urethral anomalies in boys. Part I: posterior urethral valves. Urol J. 2005; 2:59–78. [PubMed: 17629874]
6. Williams CR, Perez LM, Joseph DB. Accuracy of renal-bladder ultrasonography as a screening method to suggest posterior urethral valves. J Urol. 2001; 165:2245–2247. [PubMed: 11371954]
7. de Kort LM, Uiterwaal CS, Beek EJ, et al. Reliability of voiding cystourethrography to detect urethral obstruction in boys. Urology. 2004; 63:967–971. [PubMed: 15134990]
8. de Jong TP, Radmayr C, Dik P, et al. Posterior urethral valves: search for a diagnostic reference standard. Urology. 2008; 72:1022–1025. [PubMed: 18585762]
9. Robertson WB, Hayes JA. Congenital diaphragmatic obstruction of the male posterior urethra. Br J Urol. 1969; 41:592–598. [PubMed: 5383558]
10. Hoagland MH, Hutchins GM. Obstructive lesions of the lower urinary tract in the prune belly syndrome. Arch Pathol Lab Med. 1987; 111:154–156. [PubMed: 3813830]
11. Sharpe J, Ahlgren U, Perry P, et al. Optical projection tomography as a tool for 3D microscopy and gene expression studies. Science. 2002; 296:541–545. [PubMed: 11964482]
12. Sharpe J. Optical projection tomography. Annu Rev Biomed Eng. 2004; 6:209–228. [PubMed: 15255768]
13. Ritman EL. Current status of developments and applications of micro-CT. Annu Rev Biomed Eng. 2011; 13:531–552. [PubMed: 21756145]
14. Robyr R, Benachi A, Daikha-Dahmane F, et al. Correlation between ultrasound and anatomical findings in fetuses with lower urinary tract obstruction in the first half of pregnancy. Ultrasound Obstet Gynecol. 2005; 25:478–482. [PubMed: 15816021]
15. Apold J, Dahl E, Aarskog D. The Vater association: malformations of the male external genitalia. Acta Paediatr Scand. 1976; 65:150–152. [PubMed: 1258631]

16. Fernbach SK. Urethral abnormalities in male neonates with VATER association. AJR Am J Roentgenol. 1991; 156:137–140. [PubMed: 1898547]

17. Bernardes LS, Aksnes G, Saada J, et al. Keyhole sign: how specific is it for the diagnosis of posterior urethral valves? Ultrasound Obstet Gynecol. 2009; 34:419–423. [PubMed: 19642115]

18. Abbott JF, Levine D, Wapner R. Posterior urethral valves: inaccuracy of prenatal diagnosis. Fetal Diagn Ther. 1998; 13:179–183. [PubMed: 9708443]

19. Yiee J, Wilcox D. Abnormalities of the fetal bladder. Semin Fetal Neonatal Med. 2008; 13:164–170. [PubMed: 18053783]

20. Dewan PA, Keenan RJ, Morris LL, et al. Congenital urethral obstruction: Cobb's collar or prolapsed congenital obstructive posterior urethral membrane (COPUM). Br J Urol. 1994; 73:91–95. [PubMed: 8298906]

21. Osborne NG, Bonilla-Musoles F, Machado LE, et al. Fetal megacystis: differential diagnosis. J Ultrasound Med. 2011; 30:833–841. [PubMed: 21632999]

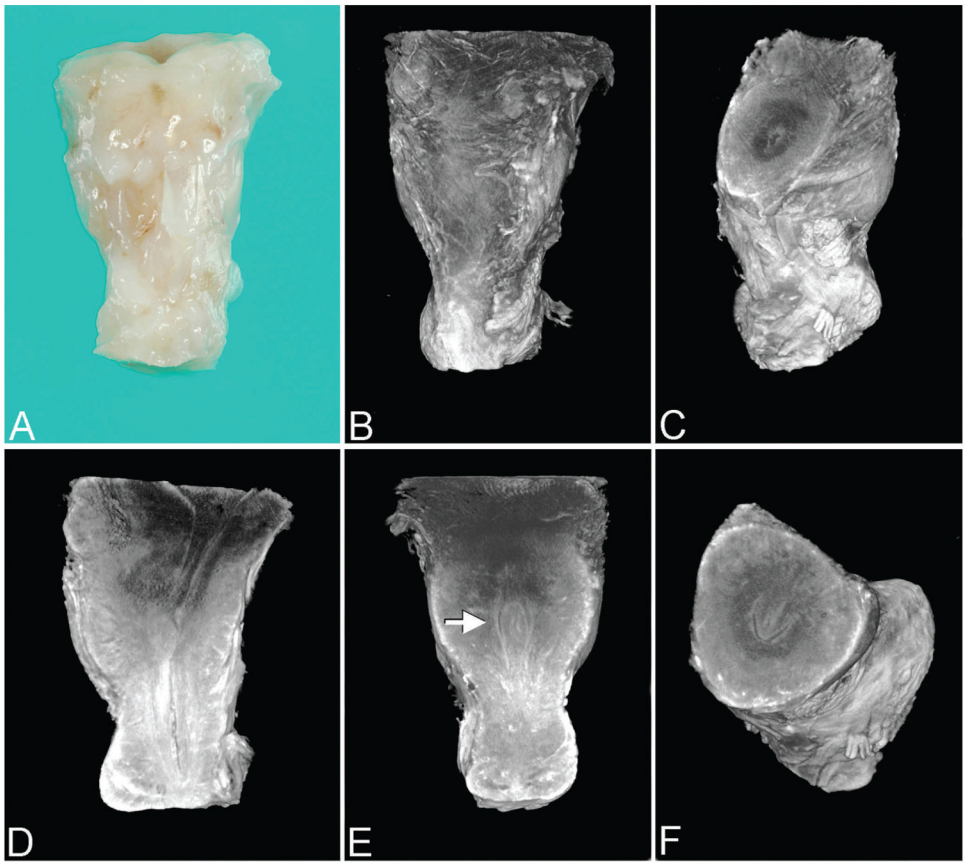

Figure 1.
Control specimen (27 weeks) imaged by optical projection tomography. Note: All images are presented in the anatomic position unless otherwise specified. **A.** Anterior surface of urinary bladder outlet and proximal-most penile shaft (gross specimen). **B.** Same orientation as **A. C.** Virtual dissection with superior-oblique view of bladder outlet. **D.** Lateral view of bladder outlet and lumen of posterior urethra. **E.** Anterior view of posterior urethra with verumontanum (arrow). **F.** Superior-oblique view of verumontanum showing prostatic utricle centrally and U-shaped urethral lumen (normal at this level). A color version of this figure is available online.

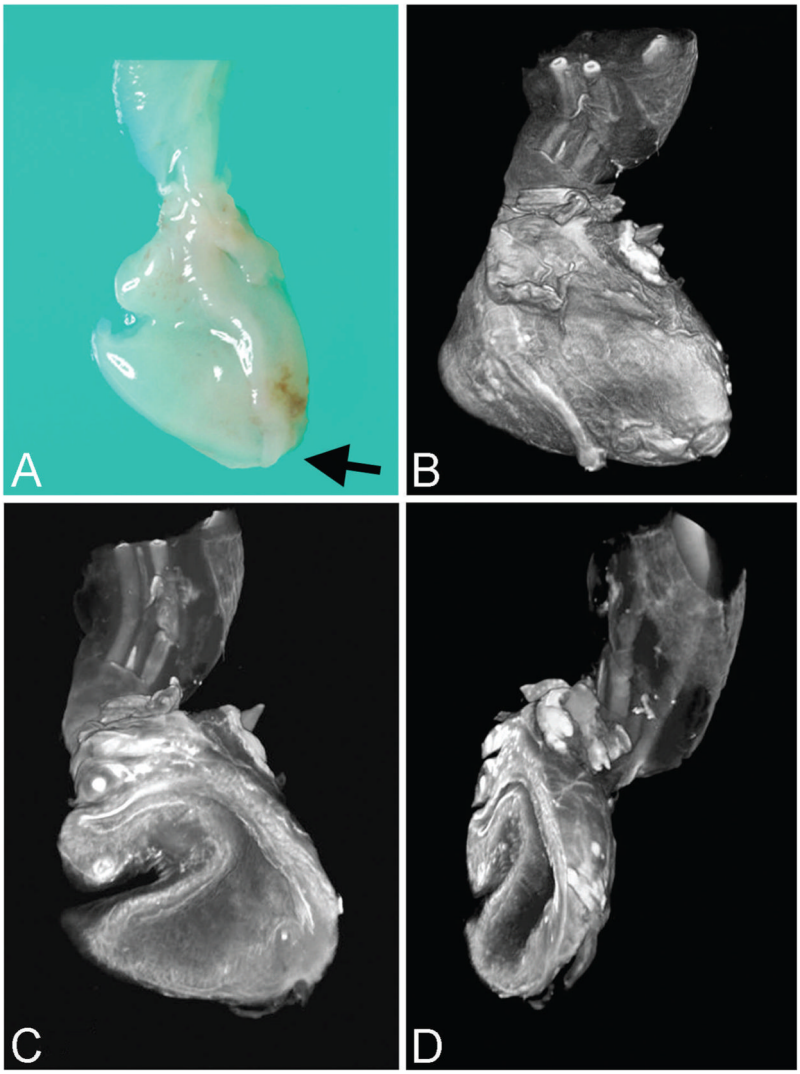

Figure 2.
Urethral atresia imaged by optical projection tomography (case 1). **A.** External view of disrupted urinary bladder without urethral orifice (arrow marks atretic region) and portion of umbilical cord and umbilical arteries at top of image (gross specimen). **B.** Same orientation as **A. C.** Virtual section of bladder interior with patent urachus (left) and cord vessels at top of image. **D.** Oblique view of bladder interior showing bladder wall without urethral orifice. A color version of this figure is available online.

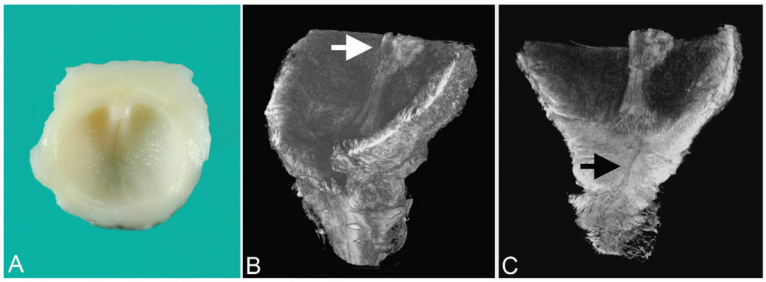

Figure 3.
Type III posterior urethral valve (urethral diaphragm) imaged by optical projection tomography (case 3). **A.** Gross specimen consisting of transected posterior urethra, portion of verumontanum, and inferior urethral crests extending to obstructive diaphragm. **B.** Superior-oblique view of posterior urethra showing inferior portion of verumontanum (arrow) and inferior urethral crests that lead to obstructive diaphragm. **C.** Coronal section of urethra showing same structures as **A** plus stenotic, discontinuous urethra (arrow). A color version of this figure is available online.

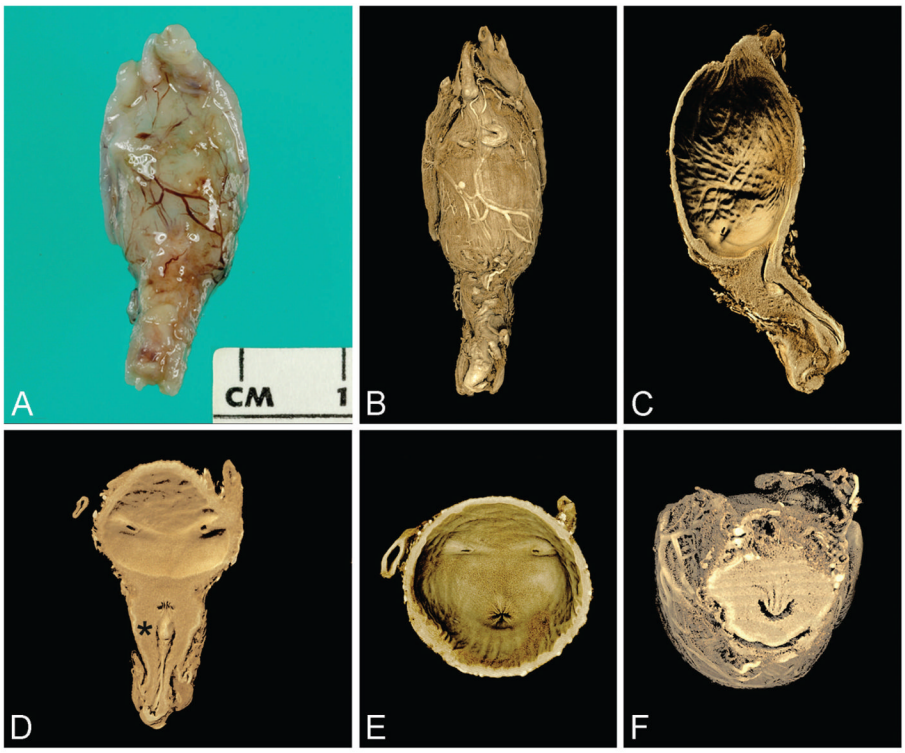

Figure 4.
Control specimen imaged by microCT (23 weeks). **A.** External view of anterior bladder with umbilical arteries present laterally and proximal penile shaft inferiorly (gross specimen). **B.** Rendered external view (same orientation as **A**). **C.** Virtual section of bladder and urethra in median plane. **D.** Virtual section of bladder and urethra in coronal plane; note insertion of ureters and verumontanum (asterisk) with inferior urethral crest. **E.** Base of urinary bladder showing urethral orifice centrally and 2 ureteral orifices laterally. **F.** Virtual section of posterior urethra in transverse plane showing verumontanum, ejaculatory ducts, and prostatic utricle (U-shaped urethral lumen is normal configuration at this level). A color version of this figure is available online. Color and shadowing are computer-generated.

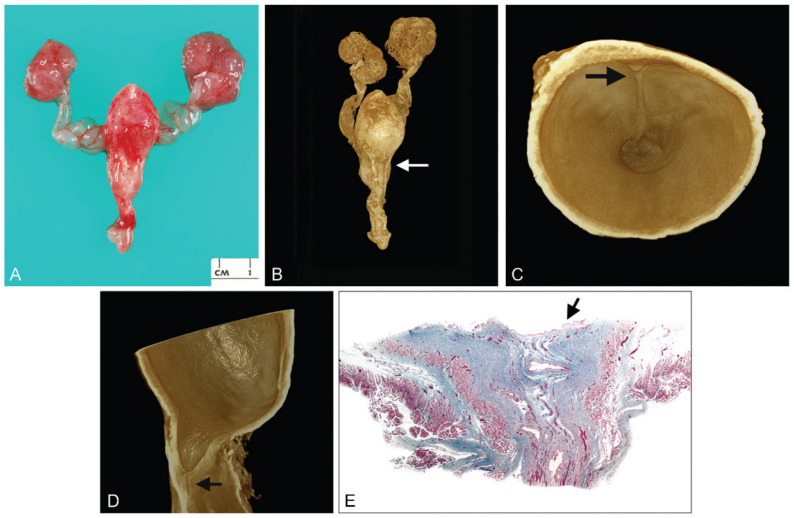

Figure 5.

Type III posterior urethral valve (urethral diaphragm) imaged by microCT (case 6). **A.** Anterior view of gross specimen showing megacystis, dilated ("keyhole") posterior urethra with penis, dilated ureters and renal pelves, and cystic kidneys. **B.** Rendered external view (cystic kidneys were bisected at autopsy) showing close correspondence to **A** (arrow marks plane of virtual section shown in **C**). **C.** Interior view of transversely sectioned dilated posterior urethra showing inferior portion of verumontanum and urethral crest (arrow) extending to obstructive diaphragm. **D.** Virtual section in median plane providing lateral view of obstructive diaphragm and stenotic distal urethra (arrow). **E.** Photomicrograph of trichrome-stained urethra showing obstructing diaphragm (arrow) and patent urethra distally (×15). A color version of this figure is available online. Color and shadowing are computer-generated.

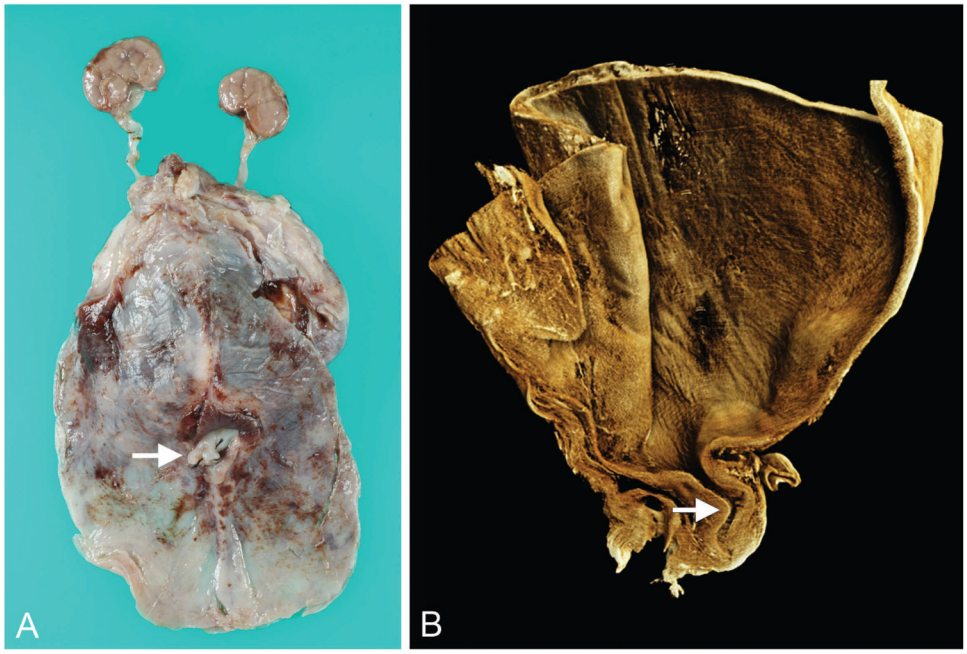

Figure 6.
Tortuous, stenotic posterior urethra imaged by microCT (case 7). **A.** Gross specimen showing massive distention of urinary bladder and mildly dilated ureters (arrow marks base of penis). **B.** Medial virtual section on rendered volume showing dilated urinary bladder and tortuous, stenotic posterior urethra (arrow). A color version of this figure is available online. Color and shadowing are computer-generated.

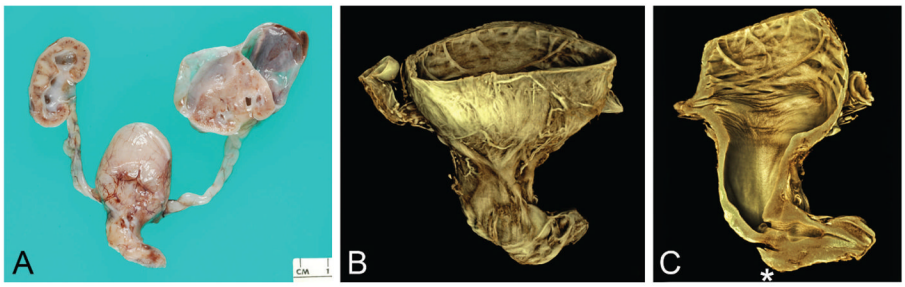

Figure 7.

Atypical kinking of posterior urethra with poststenotic dilatation and more distal obstructing diaphragm (case 10). **A.** Gross specimen showing hydronephrosis, with large perirenal cyst (urinoma), hydroureter, megacystis, dilated posterior urethra, and proximal penis. **B.** Rendered volume after microCT imaging of sectioned bladder, posterior urethra, and proximal penis. **C.** Virtual section in median plane showing dilated urinary bladder and posterior urethra; from proximal to distal, note regions of urethral stenosis followed by poststenotic dilatation, obstructing diaphragm, and patent urethra. (This distal diaphragm is consistent with a “congenital obstructive posterior urethral membrane,” or COPUM, as described by others [20].) When scanned, the lumen of the bladder/proximal urethra and lumen of the more distal urethra did not lie in the same plane; this was overcome by manually defining separate planes for the tissue with the software, the joining of which resulted in the faint oblique line visible across the stenotic urethral lumen (asterisk). A color version of this figure is available online. Color and shadowing are computer-generated.

Table 1

Microtomographic findings in bladder outlet obstruction

Case	Age	US findings	PM findings	Urethral findings by microtomography
Optical projection tomography				
1	14 W	Dilated bladder; renal pyelectasis	Megacystis; apparent atresia of proximal urethra; hydronephrosis; delivery by D&E	Urethral atresia
2	16 W	Megacystis	Megacystis; dilated posterior urethra with urethral atresia; delivery by D&E after IUFD	Urethral atresia
3	39 W	Megacystis; ascites and pleural effusions	Megacystis; dilated posterior urethra; “posterior urethral valves”	Type III PUV (obstructive diaphragm)
MicroCT				
4	17 W	Dilated bladder with inferior keyhole appearance; echogenic kidneys with pyelectasis; ascites	Dilated urinary bladder; paucity of renal tubules and possible collapsed cysts; delivery by D&E	Urethral atresia
5	19 W	Enlarged bladder with keyhole appearance; echogenic kidneys with small cysts	Megacystis; dilated posterior urethra; obstructed urethral orifice; cystic renal dysplasia; delivery by D&E	Urethral atresia
6	19 W	Thickened bladder wall with inferior keyhole appearance; hydroureter	Megacystis; hydroureter; proximal urethral diaphragm	Type III PUV (obstructive diaphragm)
7	25 W	No prenatal care	Prune belly, phenotype, with massively distended abdomen, ascites, and hypoplastic abdominal muscles; megacystis with urethral obstruction; hydroureter; hydronephrosis	Tortuous, stenotic posterior urethra
8	31 W	Postnatal US: enlarged bladder; reproductive organs not identified in genital region, inguinal canals, or pelvis	Urethral stenosis; atypical insertion of ureters and R-V fistula (VACTERL)	Severe urethral stenosis; ectopic seminal vesicles and insertion of ureters (at dome of bladder)
9	21 W	Distended abdomen with cystic mass of uncertain location	Hydroureter; hydronephrosis; urethral atresia	Keyhole dilatation of posterior urethra, with urethral atresia
10	22 W	Enlarged bladder; keyhole appearance of posterior urethra	Megacystis; keyhole dilatation of posterior urethra with probable atresia	Megacystis; kinking of dilated posterior urethra with associated stenosis; mild poststenotic dilatation of urethra with obstructing diaphragm (COPUM) in distal-most urethra

US indicates ultrasound (prenatal unless designated otherwise); PM, postmortem; W, weeks gestation; D&E, dilatation and extraction; IUFD, intrauterine fetal demise; PUV, posterior urethral valves; R-V, rectovesical; VACTERL, association of vertebral, anal, cardiac, tracheo-esophageal, radial or renal, and limb anomalies.

Table 2

Correlation of microtomographic and light microscopic findings

		Light microscopic findings	
Case	**Microtomographic findings**	**Urethra**	**Prostate**
Optical projection tomography			
1	Urethral atresia	Microtomography confirmed	None identified
2	Urethral atresia	Microtomography confirmed	None identified
3	Type III PUV (obstructive diaphragm): urethra patent distal to diaphragm	Slit-like urethral lumen in diaphragm; urethra patent distal to diaphragm	Hypoplastic, displaced inferior to verumontanum
MicroCT			
4	Urethral atresia	Severe urethral stenosis	None identified
5	Urethral atresia	Microtomography confirmed	None identified
6	Type III PUV (obstructive diaphragm)	Microtomography confirmed	Hypoplastic, adjacent to diaphragm
7	Tortuous, stenotic posterior urethra without keyhole dilatation	Microtomography confirmed	Hypoplastic
8	Severe urethral stenosis; ectopic seminal vesicles and insertion of ureters (at dome of bladder)	Microtomography confirmed	None identified
9	Keyhole dilatation of posterior urethra, with urethral atresia	Microtomography confirmed	None identified
10	Megacystis; kinking of dilated posterior urethra with associated stenosis; mild poststenotic dilatation of urethra with obstructing diaphragm (COPUM) in distal urethra	Microtomography confirmed	Hypoplastic

PUV indicates posterior urethral valves; COPUM, congenital obstructive posterior urethral membrane.

Table 3

Comparison of optical projection tomography and microCT

	OPT	microCT
Specimen preparation	Involved	Easier
Imaging modality	White, infrared, ultraviolet	X-ray
Specimen size	1.7 × 2.5 cm	20 × 6.8 cm
Resolution	1–35 μ	9, 18, 35 μ
Scan time[a]	5–20 min	5–45 minutes
File size[a]	300 MB–2 GB	600 MB–10 GB
Quantitative analysis	Yes	Yes
Postscan histology	Yes	Yes
Special stains possible	Yes	No
Expense[b]	$120 000	$300 000

OPT indicates optical projection tomography.

[a] Scan time and file size depend upon size of specimen and desired resolution.

[b] Approximate cost in U.S. dollars (includes scanner and supporting computer hardware and software).